

Dynamic features in the solar atmosphere with unusual spectral line enhancements and Doppler-shifts

J.G. Doyle¹, B. Ishak¹, M.S. Madjarska^{2**}, E. O’Shea¹, and E. Dzifčáková³

¹ Armagh Observatory, College Hill, Armagh BT61 9DG, N. Ireland

² Royal Observatory of Belgium, 3 Circular Avenue, B-1180 Brussels, Belgium

³ Astronomical Institute, Faculty of Mathematics, Physics and Informatics, Comenius University, Mlynská dolina, 842 48 Bratislava 4, Slovakia

**now at: Max-Planck-Institut für Sonnensystemforschung, Max-Planck-Str. 2, 37191 Katlenburg-Lindau, Germany

ABSTRACT

Context. The solar atmosphere contains a wide variety of transient features, here, we discuss data relating to one such feature.

Aims. To explore via simultaneous spectral and imaging data the nature of high-velocity flow events in the solar transition region.

Methods. High spectral and temporal resolution data from SUMER/SoHO plus high resolution images from TRACE are used.

Results. In the transient feature discussed, we see a factor of two enhancement in N v 1238, coupled with a factor of two decrease in O v 629 visible over 3''–4'' along the slit. Furthermore, the O v line shows a secondary component with a down-flow of $\approx 75 \text{ km s}^{-1}$, while the N v line shows only a small additional broadening of the line.

Conclusions. Inclusion of an electron density dependent ionization calculation will increase the N v radiance over that of O v at large electron densities. We suggest this feature can be explained via a highly focused jet at the O v/OvI formation temperature resulting from reconnection. Also, we believe that this event is not unique but that their detection depends on the availability of simultaneous spectral and imaging data of comparable spatial and temporal resolution.

Key words. Sun: activity – Sun: UV radiation – Sun: transition region – Sun: atmosphere – Sun: corona – Atomic processes

1. Introduction

Over the last decade the uninterrupted, high resolution coverage of the Sun both from the excellent range of telescopes aboard many spacecraft and from ground-based instruments has led to a wealth of observations of small-scale dynamic events observed from the chromosphere to the transition region and corona. Over the past few years, many complicated and dynamic fine structures have been reported in association with the network boundaries, e.g., bi-directional jets (sometimes called ‘explosive events’), blinkers, network flares and bright points. However, their interpretation, interrelationship and relationship to the underlying photospheric magnetic concentrations remains ambiguous, because the same feature has a different appearance when observed in different spectral lines and with different instruments. For example, evidence has been presented by O’Shea et al. (2005) and Madjarska et al. (2006) showing that macro-spicules and blinkers may be the same feature. Harrison et al. (2003) in an attempt to unify some of these phenomena found that a number of events such as blinkers, network and cell brightenings and EUV brightenings can be classified as the same type of phenomenon.

Doyle et al. (2005) presented data of a feature which showed a large line-shift in the N v 1238 Å line, while it was

practically absent in O v 629 Å despite the fact that both lines have over-lapping formation temperatures, with the peak formation temperature separated by $\log T_e = 0.08 - 0.12$ (depending on the assumed atomic model).

In an effort to better understand the range of dynamic features in the solar atmosphere, we re-visit the above work, in particular to explore further multi-wavelength datasets.

2. Data Reduction

For the present study, the observations were made with the SUMER spectrograph (Wilhelm et al. 1995, Lemaire et al. 1997) onboard SoHO. SUMER is designed in such a way that it enables line profile measurements at a spatial pixel size of 1'' and a spectral pixel size of 0.042 – 0.045 Å.

The present dataset was taken within an active region on June 3 1999 from 09:17:17 UT to 11:08:02 UT. Slit 0.3'' × 120'' was used, exposing for 25 s on the bottom part of detector B (see Table 1 for the list of spectral lines observed). The temporal sequences (28 s cadence) has five spectral windows (120 spatial × 50 spectral pixels). During the observations, the solar rotation compensation mode was turned on. An overview of the active region as seen in TRACE 1550 Å at 09:58:31 UT on 3 June 1999 is shown in the bottom right panel of Fig. 1.

We applied the standard SUMER data reduction procedures in this analysis. The steps include decompressing and revers-

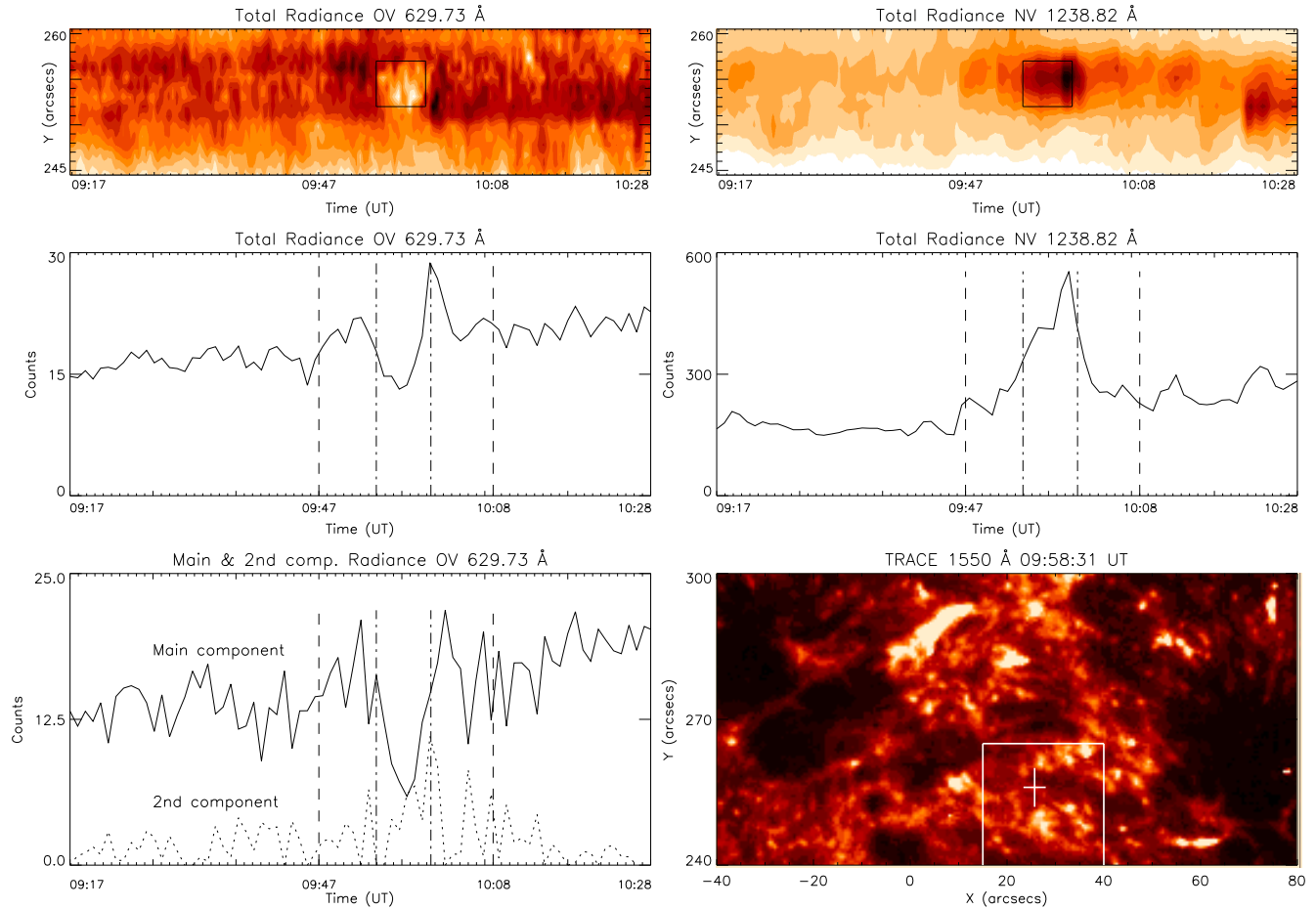


Fig. 1. (top panels) The radiance as derived for a 15'' region along the slit (averaged over ≈ 56 s) in O v 629 Å (using the main component in a two-Gaussian fit) and N v 1238 Å (assuming a single Gaussian) from 09:17:17 UT to 10:27:41 UT on 3 June 1999. (middle panel) The radiance at position 254'' along the slit in the O v (summing the main and secondary components) and N v. (bottom left panel) The radiance of the main and secondary O v component separately. The dashed and dot-dashed lines refer to intervals where we show line profiles in Fig. 2. (bottom right panel) An overview of the region as seen from a TRACE 1550 Å image taken at 09:58:31 UT with the location of interest indicated by the cross-hair. A closer view of that region as outlined by the square is shown in Fig. 3.

ing the raw data and applying a flat field correction to correct the non-uniformities in the sensitivity of the detector. Also, a geometrical distortion correction was applied so that the rest position of the line profiles are on the correct spectral pixel and the slit images are straightened. To further analyze the data set, we used a Gaussian-fitting procedure in the SolarSoft (SSW)¹ library to get the amplitude, central position, full width at half maximum (FWHM) and χ^2 of the line profiles. A small drift correction in the Doppler shift over the 110 min observations due to thermal deformations was also applied. The derived Doppler shifts are therefore relative to the mean value summed over the full observational interval. Further details on the full dataset and TRACE/SUMER co-alignment may be obtained from Doyle et al. (2006).

3. Results

The data were first inspected for transient events. One such event is shown in Fig. 1, where we show the radiance as determined from a single Gaussian line fit for N v and a double-Gaussian for O v (see below). At $\approx 09:47$ UT, we see an en-

Table 1. A summary of the spectral lines observed.

Spectral line	Comment
N v 1238.82 Å	
N v 1242.80 Å	
C I 1249.41 Å + Si x/2 624.78 Å	blend
Mg x/2 624.95 Å + Si II 1250.09 Å	blend
Si II 1250.41 Å + C I 1250.42 Å + S II 1250.58 Å	blend
Si II 1251.16 Å + C I 1251.17 Å	blend
O v/2 629.73 Å	

hancement in both O v 629 and N v 1238. At $\approx 09:53$ UT, O v starts to decrease in intensity, while N v continues to increase, becoming a factor of two stronger by $\approx 09:58$ UT. At the same time, O v shows a decrease by a similar factor. The O v and N v change in radiance is visible over 3–4 pixels along the slit.

In Fig. 2, we show the detailed line profile for both spectral lines, summed over 112 s. For N v 1238, a single Gaussian gives an excellent fit, although at 09:58:57 UT and 10:00:49 UT, the line is slightly broader. However, O v 629 requires a double Gaussian throughout the observation, with

¹ <http://www.lmsal.com/solarsoft/>

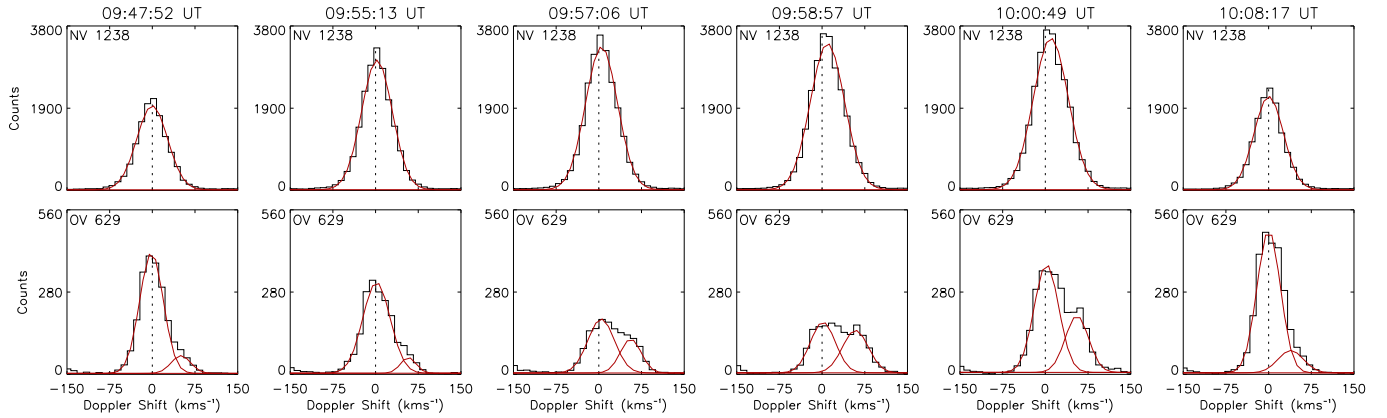


Fig. 2. Line profiles (summed over ≈ 112 s) for N v 1238 Å (top) and O v 629 Å (bottom). The first and the last profiles were taken before and after the event (at the position of the dashed lines in Fig. 1), while the four central profiles during the event at the time interval shown with dashed-dotted line in Fig. 1. The derived Doppler shifts are relative to the mean value (given by the dashed line) summed over the full observational interval.

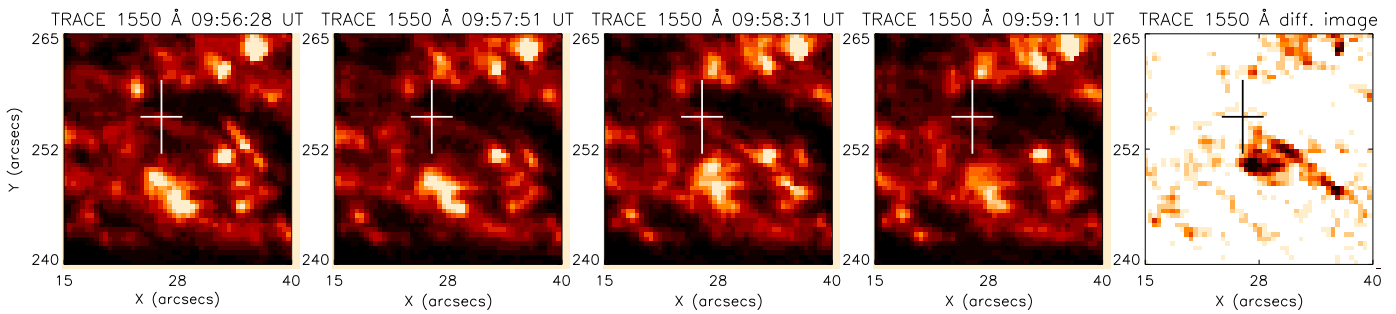


Fig. 3. The first four frames are TRACE 1550 Å images from 09:56:28 to 09:59:11 UT showing an enlarged view of the location of the transient event. Note the jet-like feature whose end-point appears at the cross-hair in the image taken at 09:58:31 UT. The jet is best seen in the fifth frame which is a reverse-color plot of the difference between the second and third frames (also see <http://www.arm.ac.uk/~jgd/movie/jet>).

the second component starting to increase in radiance after $\approx 09:55$ UT as can be seen in the second and third frames. The trend of increasing N v versus a decrease in O v is obvious, with the O v showing an increase in radiance towards the end of the event for a short interval.

4. Discussion

This event is similar to that reported by Doyle et al. (2005), regarding the relative changes in the N v to O v intensities. However, in the previous paper a large line-shift was seen in N v. Here, we see the reverse, i.e. O v is shifted. As pointed out by the above authors, inclusion of a proper electron density dependent ionization calculation will increase the N v radiance over that of O v at large electron densities (this is ignored in the coronal model, e.g. Mazzotta et al. 1998). The weak Si II line to the red of O v shows a small increase in radiance while the Mg x second order line decreases, similar to O v.

In an earlier study, Doyle et al. (2003) used a non-Maxwellian electron distribution to explain how a high-velocity flow feature which was registered in both chromospheric and transition region lines, but not showing any detectable signature in a coronal line, was clearly detected by the TRACE imager with the 171 Å filter (which is normally assumed to detect plasma close to 10^6 K). Using a Kappa non-Maxwellian distribution incorporated into CHIANTI, we calculate for $\kappa = 5$ and a quiet Sun differential emission measure that N v 1238 can be enhanced by 40% compared to the

Maxwellian distribution, while O v 629 is only enhanced by 10%. Hence coupling a slight departure from a Maxwellian distribution (e.g., $\kappa = 5$) and electron density dependent ionization will enhance N v by a factor of 2-3, while O v is reduced by a factor of 1.5-2. Both the non-Maxwellian and the density dependent ionization shifts O v and N v to slightly lower formation temperatures (Doyle et al. 2003, 2005), than those from standard ionization equilibrium calculations.

In order to gain more information of this particular event, we looked at a sequence of images taken by TRACE in the 1550 Å filter. In Fig. 3 we show an enlarged area around the region of interest from 09:56:28 to 09:59:11 UT. In the images we see several small enhanced radiance concentrations, probably due to enhanced magnetic fragments, frequently seen in MDI images. In the 09:58:31 UT image, we see a jet-like feature, the end of which coincides with the determined location of the event seen in SUMER. The jet is best seen in the reverse-color image shown in the fifth frame of Fig. 3, this image being the difference between the second and third frames. Several other small intensity enhancements are stable over the 5-10 min observational interval, although the one below the cross-hair has almost disappeared by 09:59:11 UT, perhaps resulting from the fragmentation of under-laying magnetic fragments. TRACE 171 Å did not show any response at the time or location of the 1550 Å jet feature. Ryutova et al. (2003) argue that the appearance of transient features such as flows, jets,

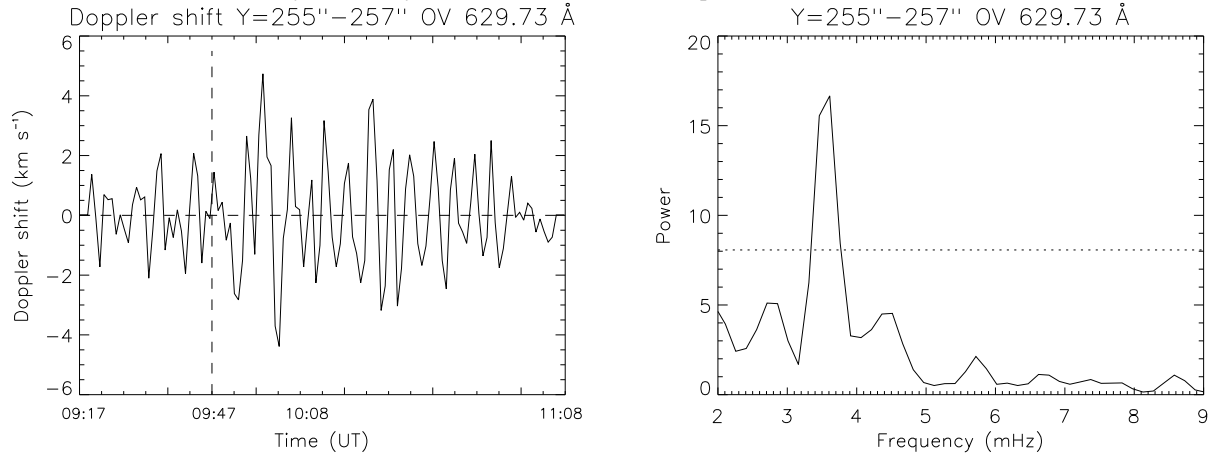


Fig. 4. The Doppler shift derived from summing pixels 255'' to 257'' over two time pixels (i.e. 56 s), plus the corresponding Fourier power and the significance level (dotted line). The dashed line refers to the start time of the feature in Fig. 1.

explosive events and blinkers, result from the collision of non-collinear flux tubes. Depending on the geometry of the shock collision and the physical parameters of the medium, this leads to magnetic reconnection at higher temperatures. For a background temperature of around 7300 K, the jet can have velocities close to 100 km s^{-1} , with the behind-shock temperature being around $1.5 \times 10^5 \text{ K}$. A similar scenario can be achieved by wave leakage of MHD waves from the lower atmosphere.

Whichever scenario is applicable, both are consistent with the TRACE 1550 Å images which shows a jet-like feature present during the timing and location of the O v Doppler shift. The decrease in the O v radiance could be due to the energy going into producing a flow of 75 km s^{-1} , as opposed to heating, while at the N v formation temperature this same flow has decreased to only a few km s^{-1} , producing only a small line broadening to the red. Given the small difference between their formation temperatures, this could suggest a very steep electron density gradient, with the density being significantly higher where N v is formed compared to where O v is formed. However, Ryutova & Tarbell (2000) suggested that cylindrical focusing could in some instances explain the presence of a jet seen in an O vi spectral line observed with SUMER, with no indication of a radiance increase in the TRACE 1550 Å filter, very similar to the present observations. This would suggest the temperature of the feature is very localized around O v.

Both physical scenarios (wave leakage and flux tube collisions) predict the presence of magneto-acoustic waves close to these jets. We searched the SUMER data for evidence of an oscillation at locations from $Y = 250''$ to $Y = 260''$. In Fig. 1, we see that the upper boundary of the event occurs around $Y = 255''$. It is only here that we see evidence for an oscillation period, and only in the Doppler-shift of the main component. In Fig. 4, we sum over $Y = 255''$, $256''$ and $257''$ and over two time pixels (i.e. 56 s) in order to increase the S/N. We see a period at $\approx 285 \text{ s}$ with the Doppler-shift varying by $\pm 2\text{--}3 \text{ km s}^{-1}$ starting after the time of the jet and lasting for $\approx 30 \text{ min}$. Summing the data over a similar number of pixels in a nearby location, we estimate the error in the Doppler-shift to be $\pm 1.5 \text{ km s}^{-1}$. To calculate the significance level, we use the procedure as in outlined in Doyle et al. (1999). Given the absence of radiance oscillations, this may suggest kink waves

resulting from the movement of small flux tubes within a 3–4'' region. These waves being perhaps activated by the collision of the jet with the surrounding region. In summary, we speculate that at the O v formation temperature, most of the energy goes to producing the jet, while at the slightly lower formation temperature of N v, the energy goes into heating. A more detailed study of a range of such features is required.

Acknowledgements. We would like to thank L. Xia, I. Ugarte-Urra, L. Teriaca, R. Erdélyi, plus the SUMER/SoHO and TRACE teams for their help, and the referee P. Hardi for helpful suggestions. SoHO is a mission of international cooperation between ESA and NASA. Research at Armagh Observatory is grant-aided by the N. Ireland Dept. of Culture, Arts and Leisure. This work was supported in part by a PRTL research grant for Grid-enabled Computational Physics of Natural Phenomena, PPARC grant PPA/G/S/2002/00020 and the Scientific Grant Agency VEGA, Slovakia, grant No.1/2026/05 CHIANTI is a collaborative project involving NRL (USA), RAL (UK), and the Universities of Florence (Italy) and Cambridge (UK).

References

- Doyle, J.G., van den Oord, G.H.J., O'Shea, E. & Banerjee, D., 1999, *A&A* 347, 335
 Doyle, J.G., Dzifčáková, E. & Madjarska, M.S., 2003, *Sol. Phys.* 218, 79
 Doyle, J.G., Ishak, B., Ugarte-Urra, I., Bryans, P. & Summers, H.P., 2005, *A&A* 439, 1183
 Doyle, J.G., Taroyan, Y., Ishak, B., Madjarska, M.S. & Bradshaw, S.J., 2006, *A&A* (in press)
 Harrison, R.A., Harra, L.K., Brković, A. & Parnell, C.E., 2003, *A&A*, 409, 755
 Madjarska, M.S., Doyle, J.G., Hochedez, A.-F. & Theissen, A., 2006, *A&A* (in press)
 Mazzotta, et al., 1998, *A&AS* 133, 403
 Lemaire, P., et al., 1997, *Sol. Phys.*, 170, 105
 O'Shea, E., Banerjee, D. & Doyle, J.G., 2005, *A&A*, 436, 43
 Ryutova, M., Habbal, S., Woo, R. & Tarbell, T.D., 2000, *Sol Phys* 200, 213
 Ryutova, M., & Tarbell, T.D., 2000, *ApJ* 541, L29
 Ryutova, M., Tarbell, T.D. & Shine, R., 2003, *Sol Phys* 213, 231
 Scherrer, P. H., et al., 1995, *Sol. Phys.*, 162, 129
 Wilhelm, K., et al., 1995, *Sol. Phys.*, 162, 189